ELSEVIER

Materials Science and Engineering A245 (1998) 72–79

MATERIALS SCIENCE & ENGINEERING A

Estimation of bainite plate-thickness in low-alloy steels

S.B. Singh, H.K.D.H. Bhadeshia *

Department of Materials Science and Metallurgy, University of Cambridge, Pembroke Street, Cambridge CB2 3QZ, UK

Received 28 April 1997; received in revised form 27 June 1997

Abstract

Published experimental data on the thickness of bainite plates in silicon-rich steels have been analysed in order to develop a quantitative model for the plate-thickness. It is found that the strength of the austenite, and the chemical free energy change accompanying transformation, are by far the most important factors influencing plate-thickness. The transformation temperature does not have any independent effect within the limits of the analysis. These trends are expected from a metallurgical point of view and are discussed in the context of the mechanism of transformation. © 1998 Elsevier Science S.A. All rights reserved.

Keywords: Bainite plates; Plate-thickness; Low-alloy steels

1. Introduction

The microstructure of bainite consists of fine plates of ferrite, growing in clusters known as sheaves. Within each sheaf, the plates are parallel and in identical crystallographic orientation, each with a well-defined crystallographic habit plane. The fine plates within a sheaf are known as sub-units. Their thickness is typically a fraction of a micrometre. Since it is the thickness rather than the plate length which primarily determines the mean free slip distance [1], there is considerable technological interest in understanding and controlling the scale of the microstructure.

There are well established trends reported in the published literature. For example, the aspect ratio (thickness/length) of sheaves is known to decrease with the transformation temperature but is not sensitive to the substitutional alloy content, at least for the low-alloy steels studied [2–4]. Other evidence has been reviewed in [5]; the general trend is that the sub-unit or the sheaf width increases as the transformation temperature is increased, whereas the number of sub-units per sheaf decreases with increasing temperature. Similar trends have been observed for martensitic transformations [6].

Like martensite, the growth of bainite causes displacements which can, on a macroscopic scale, be described by an invariant-plane strain (IPS). The invariant-plane is the habit plane of the plate [7,8]. The strain is a large shear deformation (≈ 0.26) on the habit plane and a smaller dilatational strain (≈ 0.03) directed normal to the habit plane. The magnitude of these strains is so large that the transformation product is constrained to be in the form of a thin plate, a shape which minimises the strain energy when the plate is elastically accommodated.

The shape change is not always elastically accommodated, particularly when the martensite or bainite transformation occurs at an elevated temperature where the austenite has a low yield strength. Direct observations [9] reveal the plastic relaxation in the austenite adjacent to a plate of bainite, as illustrated schematically in Fig. 1. The dislocation debris associated with the plastic deformation resists the further advance of the interface, the resistance being largest when the austenite is strong. Consequently, the strength of austenite must be an important factor in controlling the ultimate thickness of bainite plates. The plates are expected to be thicker at higher temperatures, when the yield strength of the austenite remains low in spite of the plastic relaxation. Dynamic recovery may also play a role but since this can only weaken the austenite, its effect will be similar to that of the temperature dependence of the yield strength.

On the other hand, if the austenite is sufficiently strong, then the plates are expected to be elastically

* Corresponding author. E-mail: hkdb@cus.cam.ac.uk

PII S0921-5093(97)00701-6

Table 1
The composition (wt.%) of the alloys used in the measurements of bainite plate thickness by Chang and Bhadeshia [10]

Alloy	C	Si	Mn	Ni	Cr	P	S	N
A	0.27	1.98	2.18	0.02	1.90	0.015	0.012	0.0054
C	0.46	2.10	2.15	0.02	—	0.014	0.013	0.0062
E	0.10	1.77	2.12	2.00	0.02	0.013	0.012	0.0053
F	0.26	1.85	2.10	0.02	—	0.015	0.013	0.0086
G	0.26	1.93	2.04	0.02	1.02	0.015	0.010	0.0069
H	0.10	1.63	1.99	0.03	1.97	0.013	0.011	0.0080

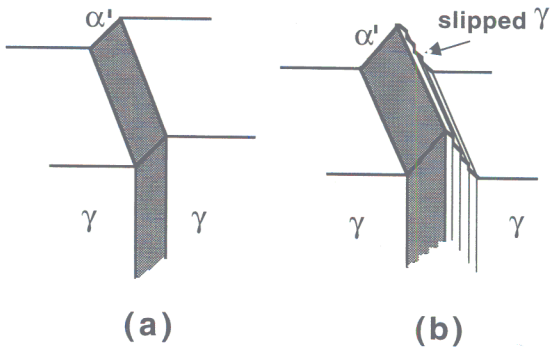

Fig. 1. Schematic illustration of a perfect invariant-plane strain surface relief (a) and one where plastic relaxation occurs in the adjacent austenite (b) [5].

accommodated. They may then maintain elastic equilibrium with the matrix, continuing to thicken until the strain energy balances the available free energy. If the plates are allowed to grow freely (i.e. without impingement) they would then be expected to be thicker at lower temperatures, where the driving force is largest. Not surprisingly, this contradicts the experimental data for bainite, which certainly is not in thermoelastic equilibrium with the matrix.

There is a further effect concerned with impingement between adjacent particles which might determine the size of bainite plates. A large nucleation rate must naturally refine the microstructure.

The purpose of the present work was to relate some recently published data [10] on the thickness of bainite sub-units to austenite strength, temperature and the chemical driving force for nucleation as independent variables.

2. Data

The bainite sub-unit data are from a set of isothermal experiments on silicon-rich steels where the precipitation of carbides is suppressed [10]. The microstructure thus consists of just bainitic ferrite and austenite, together with any martensite which forms when the austenite is cooled. The alloys that were studied are listed in Table 1.

The plate-thicknesses are listed as a function of the transformation temperature and alloy composition in Table 2. It should be pointed out that the measurements are stereologically corrected as described in [10]. The table also includes the calculated austenite strength. These calculations are based on an empirical model by Young and Bhadeshia [11], where the yield strength is expressed as follows:

$$\sigma_y^\gamma = (1 - 0.26 \times 10^{-2} T_r + 0.47 \times 10^{-5} T_r^2 - 0.326 \times 10^{-8} T_r^3 \times 15.4(4.4 + 23 w_C + 1.3 w_{Si} + 0.24 w_{Cr} + 0.94 w_{Mo} + 32 w_N), \quad (1)$$

where $T_r = T - 25$, T is the temperature in °C and w represents the concentration of the element identified by the subscript, in wt.%. The yield strength of the austenite is given in units of MPa.

The chemical free energy change (driving force) available for nucleation was calculated as in [12][1].

One difficulty is that although the strength, temperature and driving force are expected to influence the plate-thickness, the explicit dependence of the thickness on these variables is not known. The usual regression methods do not help in this respect since they require an assumed relationship to begin the analysis. We have therefore opted to conduct the regression analysis with a computer based neural network method which does not require a prior choice of the relationship between the input and output variables. The technique is introduced briefly—detailed descriptions and examples can be found elsewhere [13–18].

3. The technique

Neural networks are parameterised non-linear models used for empirical regression and classification modelling. Their flexibility makes them able to discover more complex relationships in data than traditional linear statistical models.

A neural network is 'trained' on a set of examples of input and output data. The outcome of training is a set

[1] The computer programme for these calculations can be accessed from http://www.msm.cam.ac.uk/map/mapmain.html

Table 2
The chemical free energy [12], the austenite strength [11] and the bainite plate-thickness [10] at different transformation temperatures

Alloy	Temperature °C	Free energy J mol^{-1}	Austenite strength, MPa	Bainite plate thickness, μm
A	300	−1669	121.8	0.053
	315	−1589	119.5	0.059
	330	−1503	117.4	0.083
	350	−1392	114.8	0.110
	380	−1225	111.4	0.130
	400	−1115	109.3	0.170
B	260	−2174	167.2	0.046
	270	−2104	164.7	0.055
	305	−1855	156.9	0.059
	320	−1755	153.9	0.06
	345	−1595	149.6	0.064
	370	−1454	145.8	0.093
	400	−1285	141.8	0.115
	430	−1118	138.3	0.122
E	360	−1399	75.4	0.170
	380	−1289	73.9	0.180
	430	−1015	70.8	0.210
	460	−850	69.2	0.240
F	350	−1636	108.5	0.092
	370	−1525	106.3	0.098
	400	−1358	103.4	0.120
	430	−1193	100.8	0.190
G	330	−1647	113.5	0.070
	350	−1536	110.9	0.090
	370	−1431	108.7	0.110
	400	−1254	105.7	0.120
	430	−1088	103.1	0.150
H	380	−1316	76.0	0.220
	410	−1147	74.0	0.240
	430	−1038	72.8	0.330

of coefficients (called weights) and a specification of the functions which in combination with the weights relate the input to the output. The training process involves a search for the optimum non-linear relationship between the inputs and the outputs and is computer intensive. Once the network is trained, estimation of the outputs for any given inputs is very rapid.

One of the difficulties with blind data modelling is that of 'overfitting', in which spurious details and noise in the training data are overfitted by the model. This gives rise to solutions that generalise poorly. MacKay [13–18] has developed a Bayesian framework for neural networks in which the appropriate model complexity is inferred from the data.

The Bayesian framework for neural networks has two further advantages. First, the significance of the input variables is automatically quantified. Consequently, the model-perceived significance of each input variable can be compared against metallurgical theory. Second, the network's predictions are accompanied by error bars which depend on the specific position in input space. These quantify the model's certainty about its predictions.

As described earlier, the input variables considered to influence the plate-thickness include (1) the transformation temperature, (2) the nucleation rate as represented by the free energy available for nucleation (ΔG_{max}) at the transformation temperature and (3) the strength of austenite at the temperature of transformation. The variation of elastic modulus over the temperature range considered here is negligible [19].

The variables are listed in Table 3. The plate-thickness data were available for a total of 30 combinations of temperatures and the alloys listed above. All of these were included in the analysis. The original data of Chang and Bhadeshia [10] are illustrated in Fig. 2.

Table 3
The variables used in the analysis

Variable	Range	Mean	S.D.
Temperature, °C	260–460	368.5	50.31
$-\Delta G_{max}$, J mol^{-1}	2174–850	1418	308.6
Austenite strength, MPa	69.24–167.20	112.9	29.28
Bainite plate thickness, μm	0.046–0.33	0.13	0.069

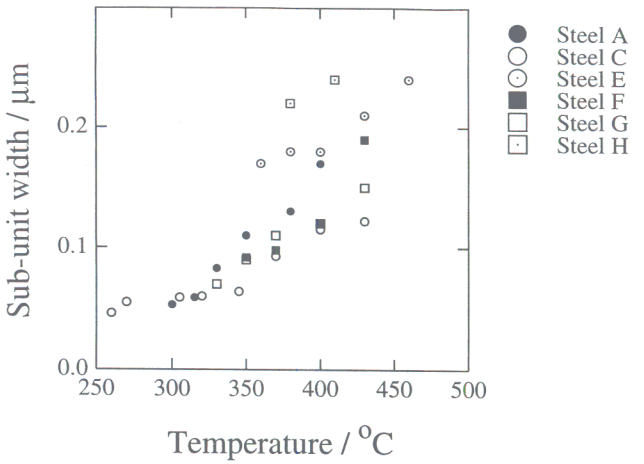

Fig. 2. The variation in bainite plate thickness as a function of transformation temperature as reported by Chang and Bhadeshia [10]. Note that a variation in the transformation temperature also causes a change in the austenite strength and the chemical driving force. Thus, the variation illustrated is not due to the effect of temperature alone.

4. The analysis

Both the input and output variables were first normalised within the range ± 0.5 as follows:

$$x_N = \frac{x - x_{min}}{x_{max} - x_{min}} - 0.5, \quad (2)$$

where x_N is the normalised value of x, which has maximum and minimum values given by x_{max} and x_{min}, respectively.

The network consisted of three input nodes, a number of hidden nodes and an output node representing the bainite plate-thickness (Fig. 3). The network was trained using a randomly chosen 15 of the examples

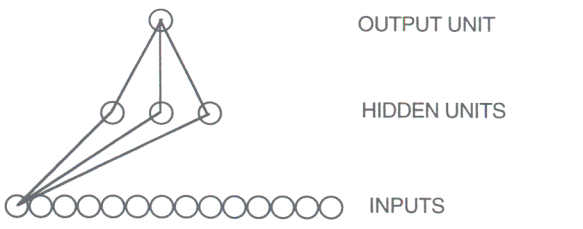

Fig. 3. A typical network used in the analysis. Only the connections originating from one input unit are illustrated, and the two bias units are not illustrated.

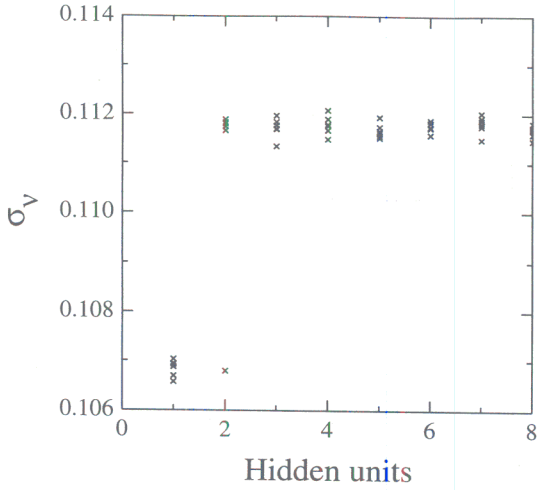

Fig. 4. Variation in σ_v as a function of the number of hidden units. Several values are presented for each set of hidden units because the training for each network was started with a variety of random seeds.

from a total of 30 available, the remaining 15 examples being kept aside at first to be used as 'new' experiments to test the behaviour of the trained network. This procedure helps avoid over-complex models.

Linear functions of the inputs, x_j, are operated on by a hyperbolic tangent transfer function[2]:

$$h_i = \tanh\left(\sum_j w_{ij}^{(1)} x_j + \theta_i^{(1)}\right) \quad (3)$$

so that each input contributes to every hidden unit. The bias is designated θ_i and is analogous to the constant that appears in linear regression. The strength of the transfer function is in each case determined by the weight w_{ij}. The 'output' y is, in the present case, the plate-thickness normalised according to Eq. (2). It can be obtained using the following linear operation:

$$y = \sum_i w_{ij}^{(2)} h_i + \theta^{(2)}. \quad (4)$$

The specification of the network structure, together with the set of weights is a complete description of the formula relating the inputs to the output. The weights are determined by training the network; the details are described elsewhere [13–18]. The training involves a minimisation of the regularised sum of squared errors. The term σ_v used below is the framework estimate of the noise level of the data. The complexity of the model is controlled by the number of hidden units (Fig. 4), and the values of the five regularisation constants (σ_w), one associated with each of the three inputs, one for biases and one for all weights connected to the output.

[2] The network operates in two stages, given by the two equations that follow. There are, therefore, two sets of w and θ coefficients. The two sets are distinguished by the superscripts (1) and (2) respectively, enclosed in brackets to avoid them being misinterpreted as exponents.

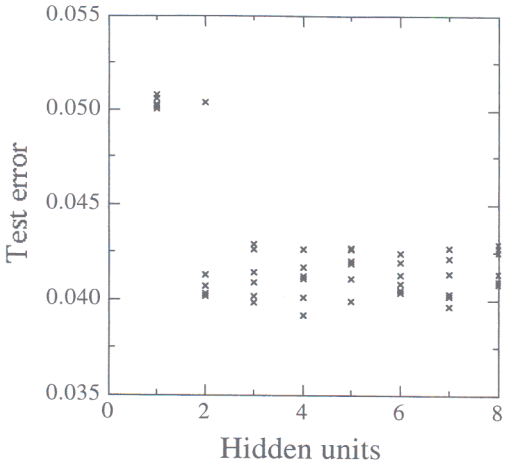

Fig. 5. The test error as a function of the number of hidden units. Several values are presented for each set of hidden units because the training for each network was started with a variety of random seeds.

The inferred noise level of the data shows little variation with the number of hidden units, Fig. 5. This can simply be because the number of data used for the training were too few. However, a highly complex model with a large number of hidden units may not be justified, because the model may, in a meaningless way, attempt to fit the noise in the experimental data. The number of hidden units was set by examining the performance of the model on the test data (Fig. 5). Even here there was only a small variation with the number of hidden units. A model with four hidden units gave the lowest test error which is a measure of the deviation of the predicted value from the experimental one. This model was then chosen to represent the variation in the bainite plate-thickness as a function of the input variables.

The agreement for the training and the test data set for the best model (4 hidden units, seed = 70) are shown in Fig. 6. The fit appears to be good and similar for both datasets, indicating again that the model is neither too simple nor too complex.

Once the optimum number of hidden units was established, the model was retrained on the entire data set to give a more accurate model. The final degree of agreement is shown in Fig. 7. The weights which would be required for the use of Eqs. (3) and (4) in order to calculate the bainite plate-thickness are listed in Table 4. The inputs and outputs are used as normalised in Eq. (2), so the maximum and minimum values listed in Table 3 are necessary in order to normalise the inputs and then unnormalise the output. The computer programme which does all these calculations is available on

http://www.msm.cam.ac.uk/map/neural/programs/plate-b.html

5. Application of the model

The model described above can be used in practice to manipulate the size of bainite plates, in general by altering the alloy chemical composition. The latter influences the austenite strength, driving force and the transformation temperatures, the effects of all of which can be estimated quantitatively using the model. For the moment we use the results of the trained model to study the effect of individual variables on the plate-thickness to see whether they make metallurgical sense.

The significance (σ_w) of each of the variables, as perceived by the neural network, in influencing the plate-thickness is illustrated in Fig. 8. The significance parameter is like the partial correlation coefficient in the multiple regression analysis. A high value of σ_w, for a given input parameter implies that this variable explains a relatively large variation in the bainite plate-thickness in the data set. Thus, it is interesting to note from Fig. 8, that a large part of the variation in the bainite plate-thickness in the data set is explained by the variation in the austenite strength. The transforma-

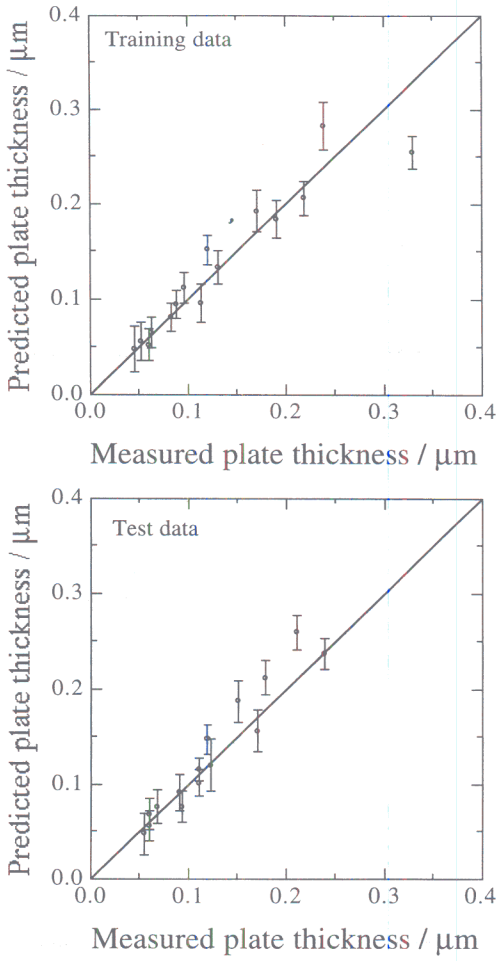

Fig. 6. (a) Training and (b) test data for the best model. The error bars represent $\pm 1\sigma$.

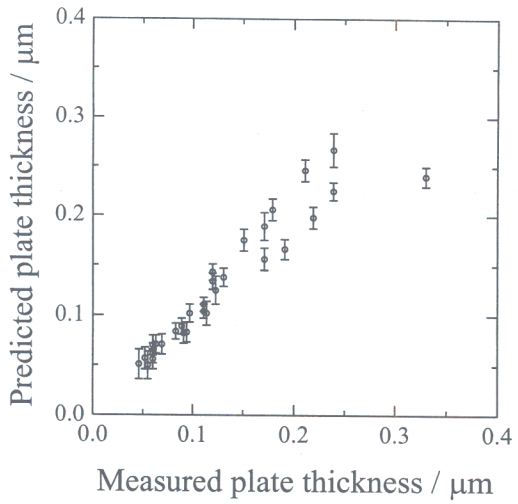

Fig. 7. Result of training on the whole data set. The error bars represent $\pm 1\sigma$.

tion temperature explains only a small part once the variation in austenite strength and driving force due to the change in temperature are allowed for separately.

The model could then be used to estimate the bainite plate-thickness given all the input variables. The effect of each individual variable is discussed below.

5.1. Effect of temperature

Fig. 9 shows the effect of temperature alone on the bainite plate-thickness at a fixed level of austenite strength and ΔG_{max}. The plate-thickness is virtually independent of the transformation temperature per se, once the austenite strength and driving force have been taken into account. Therefore, it appears that temperature by itself does not have much of an effect. This may be a reflection of the limited temperature range of the experimental data. For example, it might be expected

Table 4
The weights for the plate-thickness model

−0.00144919	−0.0024908	−0.015984	−0.0199077	0.00156831
0.00267663	0.0173535	0.0173944	−0.173165	0.0419401
0.0239065	1.38359	0.431789	−0.0746111	−0.524353
1.59167	0.141247	−0.0277307	0.0298074	0.669476
−0.952923				

The data are arranged in a continuous horizontal sequence in the following order:
$\theta_1^{(1)}, w_{1,1}^{(1)} \ldots w_{1,3}^{(1)}$
$\theta_2^{(1)}, w_{2,1}^{(1)} \ldots w_{2,3}^{(1)}$
$\theta_3^{(1)}, w_{3,1}^{(1)} \ldots w_{3,3}^{(1)}$
$\theta_4^{(1)}, w_{4,1}^{(1)} \ldots w_{1,3}^{(1)}$
$\theta^{(2)}, w_1^{(2)} \ldots w_4^{(2)}$

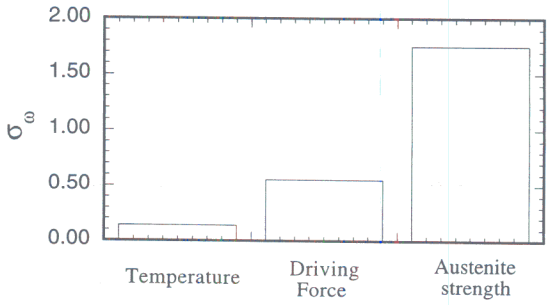

Fig. 8. The model perceived significance of the input variables in influencing the bainite plate-thickness.

that dynamic recovery effects become prominent at high temperatures in which case there would be a temperature effect which is independent of the austenite strength and the driving force.

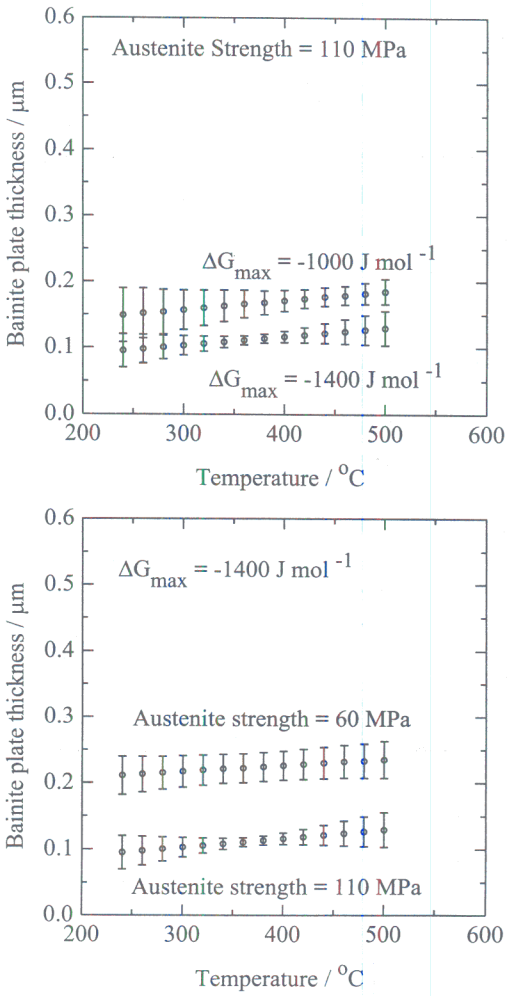

Fig. 9. The variation of the bainite plate-thickness with the transformation temperature, austenite strength and driving force. Note that unlike Fig. 2, the temperature, strength and driving force are in this illustration independent variables. The error bars represent $\pm 1\sigma$ confidence limits.

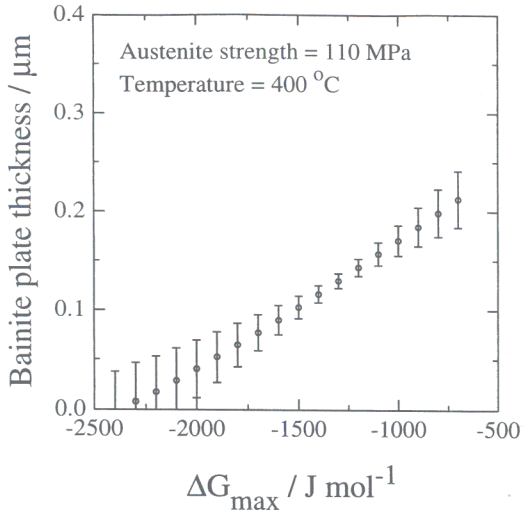

Fig. 10. The effect of driving force for bainite nucleation on plate thickness. The error bars represent $\pm 1\sigma$ confidence limits. Driving forces as large as -2500 J mol^{-1} are not expected for the transformation temperature of 400°C, but the calculations are nevertheless presented for interest.

5.2. Effect of driving force

For a given alloy composition, the driving force available for nucleation of bainite increases as the supercooling below the bainite start temperature is increased. A large nucleation rate is expected at large supercoolings (low temperatures). This must lead to a refinement of microstructure by impingement effects. Such a trend is indeed found, as illustrated in Fig. 10. It is emphasised that the model developed is nonlinear with four hidden units, capable of capturing synergistic effects between the input variables. Thus, the slope of the curve in Fig. 10 may be somewhat different for weaker austenite or for a different temperature.

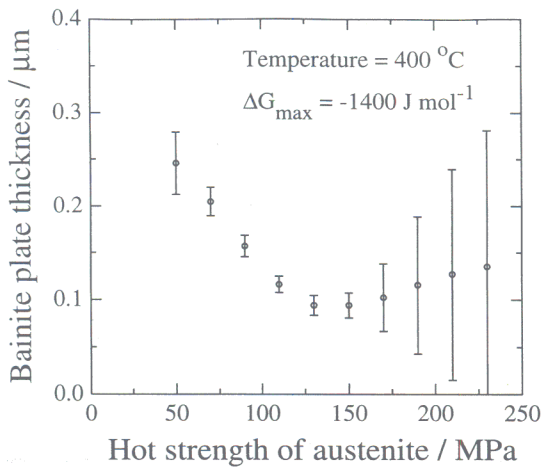

Fig. 11. The effect of austenite strength at the transformation temperature on the bainite plate thickness. The error bars are $\pm 1\sigma$ confidence limits.

5.3. Effect of austenite strength

As described earlier, for cases where the shape deformation causes plastic relaxation, weaker austenite will present a smaller resistance to interface propagation. The plate-thickness in this limit is therefore expected to decrease with increasingly strong austenite. The model perceives such a relationship, as illustrated in Fig. 11. The fact that the error bars become very large beyond ≈ 170 MPa is a reflection of the upper limit of the strength in the experimental database and the fact that the dataset itself is limited to just 30 points.

6. Conclusions

It appears that the thickness of bainite plates in silicon-rich alloys depends primarily on the strength of the austenite at the transformation temperature, and the chemical free energy change accompanying transformation, when these variables are treated independently. This conclusion applies specifically when the shape deformation causes plastic strain in the adjacent austenite. Strong austenite or a large driving force results in finer plates, the former because there is a larger resistance to interface motion and the latter because an increased nucleation rate leads to microstructural refinement.

Temperature does not, in its own right, seem to have a significant effect over the range 260–460°C, but it is possible that this situation could change should dynamic recovery effects become prominent.

Acknowledgements

The authors are grateful to the Cambridge Commonwealth Trust for a Nehru Scholarship, to British Steel for some financial support, and to Professor A.H. Windle for the provision of laboratory facilities at the University of Cambridge. HKDHB is grateful to the Royal Society for a Leverhulme Trust Senior Research Fellowship.

References

[1] J. Daigne, M. Guttmann, J.P. Naylor, Mater. Sci. Eng. 56 (1982) 1–10.
[2] G.R. Speich, in: V.F. Zackay, H.I. Aaronson (Eds.), Decomposition of Austenite by Diffusional Processes, Interscience, New York, 1962, pp. 353–386.
[3] K.J. Irvine, F.B. Pickering, Physical Properties of Martensite and Bainite, Iron and Steel Institute Special Report 93, London, 1965, pp. 110–125.
[4] M.J. Hawkins, J. Barford, J. Iron Steel Instit. 210 (1972) 97–105.

[5] H.K.D.H. Bhadeshia, Bainite in Steels, Institute of Materials, London, 1992, pp. 1–458.
[6] G. Ghosh, V. Raghavan, Mater. Sci. Eng. 79 (1986) 223–231.
[7] G.R. Srinivasan, C.M. Wayman, Acta Metall. 16 (1968) 621–636.
[8] T. Ko, S.A. Cottrell, J. Iron Steel Inst. 172 (1952) 307–313.
[9] E. Swallow, H.K.D.H. Bhadeshia, Mater. Sci. Technol. 12 (1996) 121–125.
[10] L.C. Chang, H.K.D.H. Bhadeshia, Mater. Sci. Technol. 11 (1996) 874–881.
[11] C.H. Young, H.K.D.H. Bhadeshia, Mater. Sci. Technol. 10 (1994) 209–214.
[12] H.K.D.H. Bhadeshia, Metal Sci. 16 (1982) 159–165.
[13] D.J.C. MacKay, Neural Comput. 4 (1992) 415–447.
[14] D.J.C. MacKay, Neural Comput. 4 (1992) 448–472.
[15] D.J.C. MacKay, ASHRAE, Am. Soc. Heating, Refrigerating and Air conditioning Eng. Trans. 100 (2) (1994) 1053–1062.
[16] D.J.C. MacKay, Network Comput. Neural Syst. 6 (1995) 469–505.
[17] H. Fujii, H.K.D.H. Bhadeshia, D.J.C. MacKay, ISIJ Int. 36 (1996) 1373–1382.
[18] H.K.D.H. Bhadeshia, D.J.C. MacKay, L.-E. Svensson, Mater. Sci. Technol. 11 (1995) 1046–1051.
[19] H.I. Aaronson, M.G. Hall, D.M. Barnett, K.R. Kinsman, Scr. Metall. 9 (1975) 705–712.